Membrane Skeleton Restraint of Surface Shape Change during Fusion of Erythrocyte Membranes: Evidence from Use of Osmotic and Dielectrophoretic Microforces as Probes

Arthur E. Sowers
Department of Pathology, School of Medicine, University of Maryland at Baltimore, Baltimore, MD 21201 USA

ABSTRACT The role of the spectrin-based membrane skeleton in cell fusion was studied by following the condition-dependent diameter versus time expansion signature of the fusion zone in electrofused pairs of erythrocyte ghost membranes. Previous work showed that the presence of the dielectrophoresis-inducing alternating electric field, which is used to bring membranes into contact through pearl chain formation, had a detectable promoting effect on fusion zone expansion. Two new dielectrophoresis protocols were used in the present work to utilize this externally generated and controllable microforce field to probe the forces intrinsic to the system that drives the expansion of the fusion zone. First, fusion zones expanded to a greater diameter in a strong AC field compared to a weak AC field, and they expanded to a greater diameter if erythrocyte ghosts received a prior heat treatment (42°C, 20 min). Furthermore, flat diaphragm fusion zones broke down into open lumen fusion zones sooner (i.e., had shorter lifetimes) when they were expanding more quickly. Second, changing the AC field strength at specific times during the fusion zone expansion led to an immediate visco-elastic response. However, shifting the AC field strength to zero after 5 s of fusion zone expansion resulted in a subsequent decrease in the average fusion zone diameter. This suggests not only that the spectrin-based membrane skeleton actually tends to prevent the rounding up process but that it may be capable of generating an antirounding force, which has broad implications for the role of the membrane skeleton in cell fusion. These results are consistent with the hypothesis that flat diaphragm fusion zones induced in heat-treated membranes were very easily stretched and that membrane-based forces that control or drive the expansion process must originate from membrane area that is outside rather than inside the fusion zone. Lastly, when an outward-directed osmotic pressure-based microforce was present at the time that erythrocyte ghosts were fused, the fusion zone diameter underwent a greater expansion in the 0–1 s interval after fusion. This suggests that an osmotic pressure-based microforce can be used to experimentally calibrate the dielectrophoretic force.

INTRODUCTION

This study is relevant to two general questions in cell biology. First, how are membrane shape and mechanical function/properties controlled by the structure-function relationships within the spectrin-based membrane skeleton? Second, how does the stability of a fusion zone, containing one or more fusion pores, relate to the rounding-up process that follows membrane fusion?

The spectrin-based membrane skeleton is a protein assembly that is presumed to control erythrocyte shape and deformability properties (Elgsaeter et al., 1986; Chasis and Mohandas, 1986) and seems to be present in all nucleated cells (Bennett, 1990), including those in the plant kingdom (deRijter and Emons, 1993). Sequence substitutions or deficiencies in spectrin or spectrin-associated proteins can lead to numerous pathologies (Palek and Lux, 1983). Substantial evidence suggests that transmembrane signaling, through external binding of either wheat germ agglutinin or antibodies, leads to a rigidification of the skeleton, located on the internal side of the membrane (Chasis et al., 1985). Also, it is known that the phosphorylation level of membrane skeleton proteins is controlled by a malarial kinase and can lead to a rigidification of the membrane skeleton (Cohen and Gascard, 1992, for review). Lastly, erythrocytes can exhibit a diverse family of naturally occurring and artificially inducible shapes through shape change phenomena that are not yet fully understood (Deuticke, 1968; Bessis, 1973).

The greater focus in current studies on membrane fusion (Duzgunes, 1993a,b; White, 1992), rather than on cell fusion (Poste and Nicolson, 1978), came about after it became widely recognized that membrane fusion is the key event and must happen in order for cell fusion to occur (Knutton and Pasternak, 1979). Cell fusion is thus perceived to be a spontaneous, self-completing, and obvious or otherwise unremarkable phenomenon (Roizman, 1962) driven entirely if not exclusively by surface tension (Harvey, 1954) and restrained, as previously implied, by unidentified and uncharacterized but simple physical factors. However, in addition to these physical factors, several aspects, including the role of the membrane skeleton, are also unresolved. At the submicroscopic level, the notion that an as yet poorly understood destabilizing event leads to the generation of a fusion pore, which can either collapse out of existence or go on and continuously expand in pore diameter, has gained substantial support from real time but nonimaging methods (Oberhauser et al., 1992; Monck, et al., 1990, 1991; Spruce et al., 1991). Using light microscopy imaging methods,

Received for publication 10 April 1995 and in final form 25 August 1995.
Address reprint requests to Arthur E. Sowers, P. O. Box 489, Georgetown, Delaware 19947. Tel.: 410-706-0720; Fax: 410-706-8414; E-mail: arthures@access.digex.net.

0006-3495/95/12/2507/10 $2.00

repeated cell fusions (which follow membrane fusions induced by enveloped viruses) will cause a mass called a syncytium (Roizman, 1962) to appear. In many virology studies, syncytium formation is a major diagnostic endpoint. Although it is recognized that syncytium formation is under some control or regulation (Grimaila et al., 1992; Horvath et al., 1992; Haywood, 1991), the details are still unclear. Between the submicroscopic measurements and the macroscopic observations lies a vast gap in our knowledge.

Two recent cell fusion modeling studies from our laboratory used erythrocyte ghosts to exclude the influence of cytoplasmic elements and substantially reduce the number of participating variables. Generalizing from prior works using other systems and from our own work, it now seems that after the establishment of close contact over some shared area between two (usually spherical) cells or membranes, the induction of one or multiple fusion sites (or fusion pores) in this contact area is followed by an expansion of the fusion zone as its planar area increases (Fig. 1). Examples of electron micrographs in virus-induced fusions where this is obvious have been published previously (Knutton, 1977; Pinto da Silva et al., 1980), and they show a fusion zone ultrastructure identical to that found for electrically induced fusions (Chernomordik and Sowers, 1991). The separate identity of the two original premembrane fusion components is generally considered to be completely lost when the fusion product geometry becomes a sphere (as the "swelling" process ends). However, there is significant

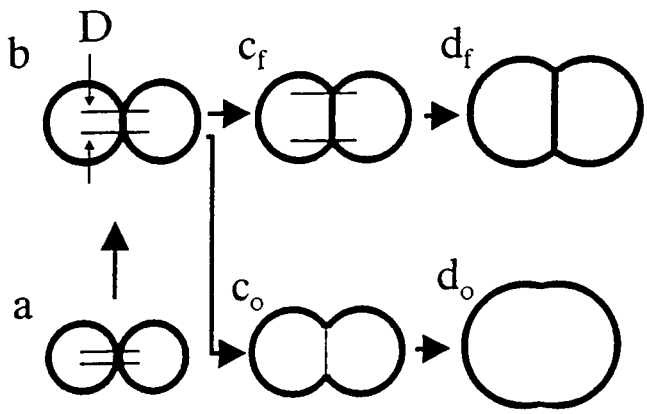

FIGURE 1 Membrane and cell fusion as it appears in phase optics in a pair of erythrocyte ghosts in close contact: a microscopic area called the "contact zone" is formed where two intact spherical erythrocyte ghosts are in close contact over a finite area defined by a circle with diameter, D (shown in a). Membrane fusion converts the contact zone into a fusion zone (containing multiple fusion pores) that visually seems to become longer (larger in diameter, D) but remains visible as a "flat diaphragm" (shown in b), which either continues to lengthen and remain visible (shown in c_f and d_f) or begins to break down into an "open lumen" by becoming thinner (shown in c_o), until it becomes undiscernible (shown in d_o). If the fusion zones are circular, then the open lumen and flat diaphragm morphologies have associated diameters. A third category (not shown) is fusogen-induced physical attachments in which pairs of membranes do not separate from one another when the dielectrophoretic field is removed but do not lead to flat diaphragms (membrane-membrane attachments seem by phase optics to be arrested as shown in a rather than b).

evidence that membrane fusion and cell fusion are experimentally separable processes (e.g., Wojcieszyn et al., 1983). In other words, cell fusion cannot happen without membrane fusion, but membrane fusion can happen without cell fusion. Also, we have observed that an "attachment" can form between erythrocyte ghosts, which does not lead to a macroscopically detectable (i.e., visible by phase optics) fusion zone (Sowers, 1988; Chernomordik and Sowers, 1991). Analogous descriptions that allow interpretations for "hemifusion" have also been recently reported (Song et al., 1991; Kemble et al., 1994) and may have a bearing on the membrane-cell fusion process. This and related issues merit additional work but are otherwise beyond the scope of the present paper.

We showed in Chernomordik and Sowers (1991) that electron micrographs of electrofused pearl chains of erythrocyte ghosts have flat diaphragm fusion zones identical to those induced by viruses (Knutton, 1977; Pinto da Silva et al., 1980) and chemicals (Ahkong et al., 1986; Lucy, 1978), suggesting that fusion zone structure is independent of fusogen type. We also showed that a prefusion or postfusion heat treatment would destabilize these flat diaphragm fusion zones so that they would subsequently become open lumen fusion zones and simultaneously allow membrane fusion products to increase in volume ("swell") toward a more spherical form. This work led us to hypothesize that fusion zones always begin as a "flat diaphragm" but could end as an "open lumen" (Fig. 1). Quantitative work, limited to pairs of electrofused ghost membranes, showed (Wu et al., 1994a) that under specific conditions the rate of expansion of the fusion zone diameter was initially high but immediately began to decrease. At ~15–20 s after membrane fusion was induced, and afterward, the expansion continued but at a more or less constant rate. When fusion was induced after certain heat treatments at specific temperatures, the observed expansions then displayed "signatures" in a manner that allowed us to clearly hypothesize a link between the change in morphology, the stability of the flat diaphragm fusion zone, and the spectrin-based membrane skeleton. Also, our observations showed that the flat diaphragm fusion zone (as visible by phase optics) could have a "lifetime" and an "expansion signature" independent of each other but could otherwise be condition-dependent (Wu et al., 1994a,b).

We also showed previously that the alternating electric field used to align the erythrocyte ghosts into pearl chains caused the fusion zone expansion rate to be measurably higher and was approximately in proportion to the strength of the field (Wu et al., 1994a). Further work provided four additional lines of experimental evidence (involving correlations with glycerol suppression of thermal sensitivity, sensitivity to agents known to target skeleton components, pH sensitivity of band 3-ankyrin associations, and the ionic strength dependence of the spectrin calorimetric transition) to support the hypothesis that the spectrin-based membrane skeleton participates in a major way in the control of the fusion zone expansion process (Wu et al., 1994b). The use

of the electrofusion protocol to induce fusion, as opposed to the use of a biological fusogen such as a virus or a chemical fusogen like polyethylene glycol, also has many distinct advantages. Electrofusion can consistently induce high fusion yields, thus making practicable studies at the single cell level. The use of an electric pulse as a fusogen avoids potential complicating or secondary effects from a chemical or a biological interaction. Lastly, when an electric pulse is used to induce fusion, the same pulse makes it possible to simultaneously fix an initial instant in time for fusion event lifetime measurements and to synchronize (time resolve) subsequent observed parameters. Overall, this approach permits membrane-membrane contact, membrane fusion, membrane type, and buffer composition to be manipulated independently.

The purpose of this paper is to report four findings. First, the rate of fusion zone expansion was highly sensitive and responsive to changes in externally generated forces from dielectrophoretic field strength (rate changes were observable within ~1 s). Second, a weak transmembrane osmotic pressure difference (hyperosmolar inside) can accelerate fusion zone expansions in fusions of nonheat-treated (= control) ghost membranes. Third, the membrane skeleton has a slight but natural tendency not only to resist but possibly also to reverse the rounding up that would take place in cell fusion. Fourth, membrane area in unstable flat diaphragm fusion zones is not likely to be a significant source of the force that restrains the rounding-up process. These results may have broad implications for how syncytium formation is regulated and may help identify, qualitatively, the force components and their relative strengths.

MATERIALS AND METHODS

Erythrocyte ghost preparation

With the following exceptions, the isolation of (pink) rabbit erythrocyte ghosts, the heat treatment, and the electrofusion of pairs of these ghosts were carried out essentially as previously described (Wu et al., 1994a,b; for reviews, see Sowers, 1992, 1993). Unless specified otherwise, all protocols were carried out at 0–4°C and involved rabbit erythrocyte ghosts suspended in 20 mM sodium phosphate (NaPi) buffer (pH 8.5). Erythrocyte ghosts were loaded with 10 kDa FITC-dextran (stock no. FD-10S, Sigma, St. Louis, MO) as follows. Rabbit erythrocytes hemolyzing in NaPi (5 mM, pH 8.5) with EDTA (1.0 mM) present for 20 min were then pelleted (10,000 × g, 20 min) and resuspended in a buffer containing FITC-dextran (3 or 6 mM) and NaPi (5 mM, pH 8.5) and then incubated for 30 min. One volume of buffer containing FITC-dextran (3 or 6 mM) and NaPi (35 mM, pH 8.5) was added to this suspension and allowed to sit at 20–22°C for 1 h. This suspension was then pelleted and resuspended with FITC dextran-free 20 mM NaPi (pH 8.5) and stored at 0–4°C until used in the fusion assay either with or without a prior heat treatment. Erythrocyte ghosts were exposed to a heat treatment (42°C for 20 min) and then returned to 0–4°C and stored at that temperature until the fusion zone measurements were carried out (at 20–22°C). The level of reloading of erythrocyte ghosts with FITC-dextran was assessed by comparing a visual estimate of fluorescence (in the fluorescence mode) with actual sedimentation rates measured by following the change in z-axis focus position (in the phase optics mode) of individual ghosts in a suspension under the microscope over time intervals ranging from 5 to 10 min and calculating sedimentation rates from calibrated points on the focus knob and time intervals measured by a stopwatch.

Dielectrophoresis protocol

In prior work from this laboratory, the alternating electric field (continuous, sine wave, 60 Hz) with the voltages used in the electric field reported as the root-mean-square value used to align erythrocyte ghosts into pearl chains was continuously present at a constant level either before or during the 120-s interval after the fusogenic electric pulse was applied to fuse the aligned erythrocyte ghosts. In contrast, two new protocols were used in the present work. First, fusion zone expansions were followed in fusions of both heat-treated and nonheat-treated (control) ghosts using an alternating electric field of 3.5 V/mm or 8.0 V/mm, which was continuously present at a constant level both before the pulse and throughout the measurements after the pulse. Second, fusion zone expansions in fusions of heat-treated ghosts had an alternating electric field of 4.0 V/mm continuously present and at a constant level before the application of the fusogenic pulse. At the pulse, the AC field strength was 1) shifted to 8 V/mm until 10 s after membrane fusion, then shifted to 4 V/mm; 2) shifted to 8 V/mm until 5 s after membrane fusion was induced, then shifted to zero V/mm; and c) continued at 4 V/mm until 30 s after membrane fusion, then shifted to 8 V/mm. Field strength "shifts" are specified as follows. The AC field strength was changed at a given time after the fusogenic pulse by two high-voltage mechanical reed relays (Stock W102VX-49, Magnecraft, Northbrook, IL), which could switch from one AC source to a second AC source. These two relays were in turn controlled by a third relay. Mechanical lag and contact bounce in these relays introduced a delay of ~50 ms between one AC field strength and a second AC field strength. This delay was considered to be insignificant in length compared with any of the $5–10^{-30}$-s subperiods of observation in the entire 120-s interval. This delay introduces a discontinuity in the data of at most only three to four video frames. A timing protocol was used to control the time interval between the pulse and the shift from one postpulse AC field strength to another. It should be noted that the pulse generator, which included the first AC source, was free of waveform "transients" because it used a resistor network and a contact bounce-free thyratron rather than a mechanical relay to control the DC pulse and AC source (see Sowers, 1989). The DC pulse produced in the fusion chamber an exponentially decaying field pulse of E = 600 V/mm with a decay half-time of 0.55 ms. Flat diaphragm fusion zone lifetimes were estimated upon playback of video sequences. During playback, the midpoint between the moment at which the flat diaphragm began to fade out of distinctness and the moment at which the flat diaphragm was no longer discernible was taken and used with the moment at which membrane fusion was induced to define the flat diaphragm lifetime.

Measurement populations

Fusion zone diameter was measured as a function of time in each of $10 < N < 30$ useful fusions, and average values were calculated from all measurements over the entire observation interval. Brownian motion-induced drift or thermal drift sometimes led to an uncontrollable loss of fusion product position from focus, thus rendering unusable the data for ~15–30% of the fusions.

RESULTS AND DISCUSSION

Overview

Although a complete biomechanical analysis is beyond the scope of this paper, we present the following hypothetical framework as a point to begin the identification and quantification of the participating forces. Work from our laboratory (Wu et al., 1994a) showed that the fusion zone diameters in fusions of control or 42°C heat-treated membranes underwent an initial rapid increase with time and then a further but slow increase, which was at a constant rate

for the 20–120 s observation period of the expansion (evaporation from the chamber prevented us from making long-term observations, and 120 s was taken as the cut-off point). A temperature of 42°C was used because it is about half way through the spectrin calorimetric transition. Had the heat treatment temperature passed all the way through the spectrin calorimetric transition (i.e., ≥45°C), fusion zone expansions would have ended in one large sphere within 1–2 s (see Fig. 3 in Wu et al., 1994a). This and related observations led us to conclude (Wu et al., 1994b) that an undenatured (nonheat-treated) membrane skeleton is actually responsible for a major control and restraint of the fusion zone expansion. These studies showed that electrofusions of nonheat-treated ghosts lead almost exclusively to flat diaphragm fusion zones, whereas electrofusions of heat-treated ghosts lead to unstable flat diaphragm fusion zones, which have lifetimes that are characteristically independent of fusion zone diameter versus time curves. Hence, our strategy was to partially perturb rather than totally denature the spectrin-based membrane skeleton to still have some influence from it as well as to examine the effects on two observables: 1) flat diaphragm lifetime and 2) fusion zone expansion signature. Although this finding is qualitatively consistent with the rounding up that is common in the cell fusion literature, it is not obvious why the expansion curves should have linear portions. Most of the curvature of each member ghost membrane in all of the fused pairs of ghost membranes remained spherical throughout the observation interval (120 s) as the fusion zone increased in diameter (Wu et al. 1994b). These observations imply that the expansion of a fusion zone is caused by a net outward force, F^o, which is stronger than the net inward force, F^i, with each shown to act at one point, the edge of the fusion zone, as shown in Fig. 2.

Our earlier work (Wu et al., 1994b) provided preliminary qualitative estimates for several anticipated force components involved in controlling fusion zone expansion. Thus, our data allowed us to argue that the drag forces (i.e., the inward-directed force components that have the effect of restricting or restraining the expansion process) from 1) viscosity of the aqueous medium, 2) membrane permeability, and 3) membrane hydration effects should be insignificant or otherwise not be rate-limiting. Second, because the expansion signature was sensitive to the ambient temperature during the measurements (Fig. 4 in Wu et al., 1994a), it was concluded that the drag from the viscosity of the membrane could be substantial. Third, it was found that fusion zone expansions took place at a higher average rate in the presence of AC fields with higher strengths. This suggested that the externally generated dielectrophoretic field was producing a force that was probably in the same order of magnitude as the net sum of all forces intrinsic to the membrane, which was driving the expansion. However, the acceleration from dielectrophoresis also suggested that dielectrophoresis itself could be used as a convenient and easily controllable microforce to probe the expansion signature if it could be calibrated or calculated. A recent study by Foster and Sowers (1995) showed that valid quantitative estimates of the strength and direction of the forces generated by dielectrophoresis on a fused membrane doublet can be obtained from theory by numerical methods and that these estimates are consistent with the experimental observations in this paper.

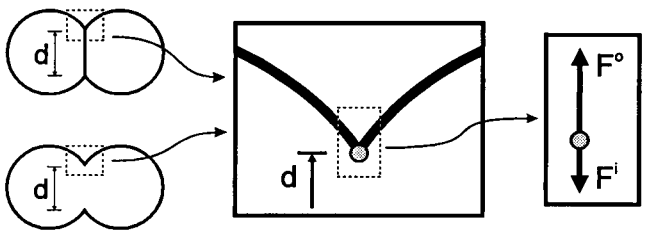

FIGURE 2 Illustration of two net resultant forces acting on a pair of fused erythrocyte ghosts. The edge of fusion zone (*left*) was at a junction either with a flat diaphragm (*upper*) or with an open lumen (*lower*) fusion zone. The junction of the two original membranes (*middle*) move toward an increasing fusion zone diameter if the net outward force, F^o, exceeds the net inward force, F^i (*right*).

Effect of constant high (8 V/mm) or low (3.5 V/mm) dielectrophoretic force throughout the expansion

In fusions of control (no 42°C heat treatment) ghost membranes, a stronger alternating electric field strength (8.0 V/mm, compared with 3.5 V/mm) caused the fusion zone diameter to expand to ~0.5 μm greater diameter by ~5 s after membrane fusion was induced. The difference in the two average diameters remained at 0.5 μm until the end of the observation period (▲ compared with ▼ in Fig. 3). In 42°C heat-treated ghosts, fusion led to a diameter increase that was dramatically (75%) greater at 60 s after membrane fusion when an AC field strength of 8.0 V/mm was used instead of 3.5 V/mm. Thus, fusions of pairs of 42°C heat-treated membranes in the presence of the higher AC field strength caused the fusion zone diameter to become much greater initially (● compared with ■ in Fig. 3) and then reached a terminal or near-terminal diameter at ~60 s after the induction of membrane fusion.

Considering that flat diaphragms (Fig. 1) in control membranes are long-lived or permanent, a small diameter expansion, compared with a large expansion, would be consistent with the hypothesis that the presence of the flat diaphragm as a physical entity produces a significant restraining force. However, as we reported previously, a heat treatment causes the flat diaphragm fusion zone to become unstable and to break down into open lumen fusion zones (i.e., the flat diaphragm lifetime becomes remarkably shorter than 120 s). However, we found (Fig. 4) that the flat diaphragm lifetimes in the fusions of 42°C heat-treated membranes were dramatically shorter in a high AC field (8 V/mm) expansion than in a low AC field (3.5 V/mm) expansion (fusions of nonheat-treated control membranes

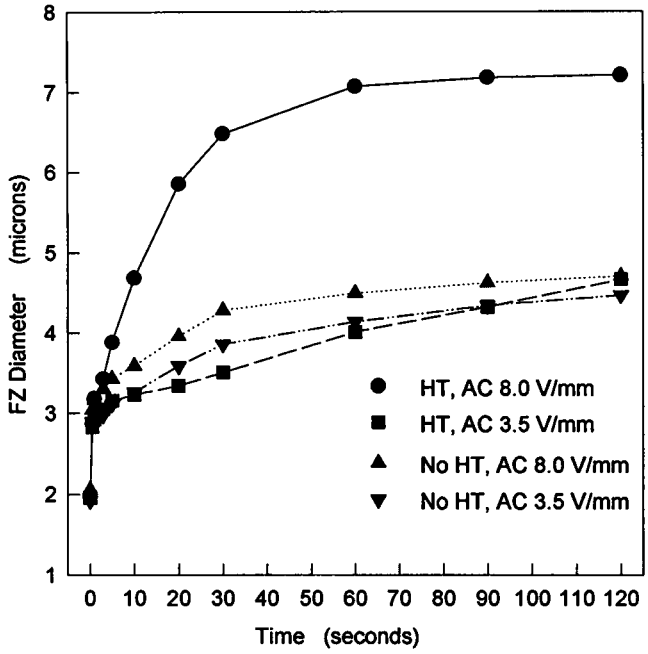

FIGURE 3 Fusion zone expansion signature in fusions of control (▲, ▼) (nonheat-treated) and heat-treated (●, ■) (42°C, 20 min) ghosts in the continuous presence of a constant low (3.5 V/mm) or a high (8.0 V/mm) 60-Hz alternating electric field present from before until 120 s after the induction of membrane fusion ($9 \leq N \leq 14$).

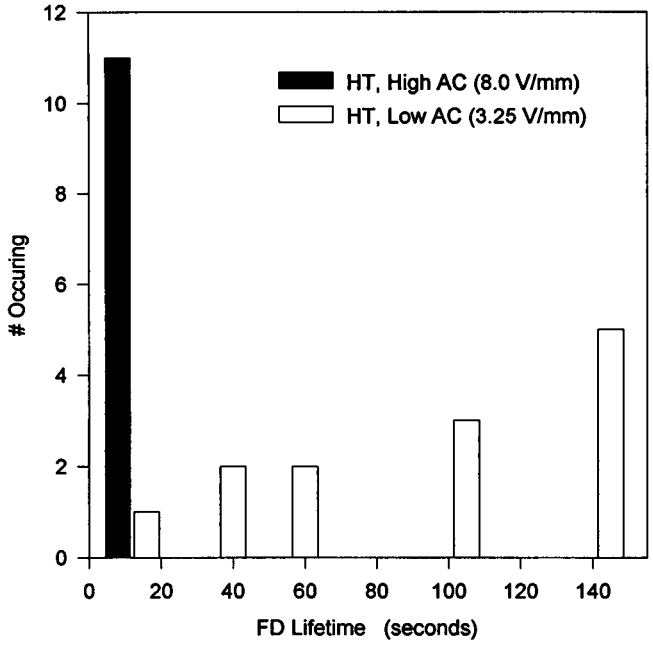

FIGURE 4 Flat diaphragm lifetime (by estimating the time midpoint of the flat diaphragm breakdown process, midway between the moment of visible diminution to the moment at which the flat diaphragm is no longer distinctly present) in individual fusions of heat-treated erythrocyte ghost membranes in the continuous presence of constant low (3.5 V/mm) or high (8.0 V/mm) 60-Hz alternating electric field, as given in Fig. 3. Note that in all 11 fusions in the high field all of the flat diaphragms broke down by the first 20 s, whereas in the 13 fusions in the low field, 8 of the flat diaphragms persisted to 60 s and 5 of those lasted to ~110 s.

resulted in flat diaphragms that were permanent over at least the 120-s observation interval). In the 8 V/mm field, all 11 flat diaphragms broke down into open lumens within 20 s, whereas in the 3.5 V/mm field only 1 of 13 flat diaphragms broke down in the first 20 s, and four additional flat diaphragms broke down by 40 s after membrane fusion. Indeed, comparison of Fig. 4 with Fig. 3 shows that the flat diaphragm lifetime, under the two different dielectrophoretic field strengths (but with the membrane preparations and the heat treatments being otherwise identical), is sensitive to stretch rate. This information allowed us to conclude that the flat diaphragm contributes an insignificant restraining force component to the expansion of the fusion zone because all the flat diaphragms had broken down by 20 s, but the fusion zone diameter continued to increase from 20 to 60 s at a continually diminishing rate rather than an increasing rate that would be expected if the flat diaphragms were restraining the expansion. In other words, if flat diaphragms were providing a significant "spring-like" (Hookian) restraining force, then that force would drop to zero as the flat diaphragm goes out of existence. If this had happened, then it would have allowed the fusion zone diameter to increase at an accelerating rate (and the average fusion zone diameter would have reached ≥ 7 μm by or before 30 s after membrane fusion was induced). Because this did not happen, it is concluded that the increase in fusion zone diameter can only be restrained by a force that must originate from the membrane area, which is outside the fusion zone. The relative force contributions from the membrane area in a long-lived flat diaphragm (as would be induced in a control = nonheat-treated pair of ghost membranes) compared with the membrane area outside the flat diaphragm cannot be assessed, however, because the flat diaphragm is always present, and we do not know the structural difference between an intact membrane skeleton and a membrane skeleton that has been carried partly through the spectrin calorimetric transition. Therefore, we cannot tell for fusions of control membranes how much of the restraining force comes from the membrane area in the flat diaphragm fusion zone versus the membrane area outside the fusion zone.

Effect of step changes in AC field strength during the fusion zone expansion

Experiments with three protocols to bring about step changes in AC field strength during the expansion of the fusion zone diameter in fusions of heat-treated membranes showed a dramatic effect on the fusion zone expansion signature (Fig. 5). From previous work (Sowers, 1983, 1986) we know that this cannot be due to an induced elevation of temperature and therefore must be happening because of generated forces. First, when the postmembrane fusion AC field was step-changed from 8.0 V/mm to 4.0 V/mm at 10 s after membrane fusion, it caused a slight

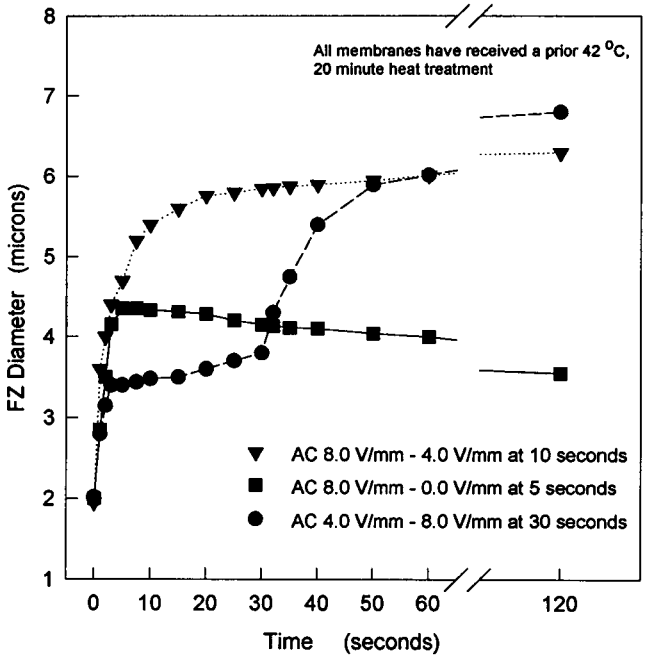

FIGURE 5 Fusion zone expansion signature in fusions of heat-treated ghost membranes aligned in a constant 60-Hz alternating field strength of 4.0 V/mm, fused with a pulse, and then the AC field was shifted, at the moment of the pulse, to 8.0 V/mm, then to 4.0 V/mm at 10 s after the fusogenic pulse (▼); immediately shifted to 8.0 V/mm, then to 0.0 V/mm at 5 s after the pulse (■); and remained at 4.0 V/mm and then shifted to 8.0 V/mm at 30 s after the pulse (●). ($10 \leq N \leq 30$).

reduction in the rate of expansion of the fusion zone diameter (▼ in Fig. 5) beginning at 10 s after membrane fusion (note that $D = 7$ μm in ● at 60 s in Fig. 3 with a constant and continuously present 8 V/mm, but $D = 6.1$ μm in ▼ at 60 s in Fig. 5 with 8 V/mm going to 4 V/mm at 10 s after membrane fusion). This is consistent with the dielectrophoretic force being (as reported in Wu et al. 1994a) in the direction of expanding the diameter. Second, the presence of an initially low AC field strength (4 V/mm from 0 to 30 s) shows that a constant restraining force involves a viscous component and/or a force component, which effectively inhibits the expansion over the range from $D = 3.3$ to $D = 3.8$ μm (● in Fig. 5), and the expansion is linear from ~3 s until 30 s after fusion, at which time the field is dramatically increased (to 8.0 V/mm). The fusion zone expansion curve then seems to follow a signature similar to ▼ in Fig. 5. This suggests that the expansion process may not have a complex hysteresis function. Third, a high field strength (8 V/mm) present from membrane fusion until 5 s later where it was shifted to zero (■ in Fig. 5), shows a rapid rise as in ▼, but as soon as the dielectrophoresis-inducing force is eliminated, the average fusion zone diameter actually undergoes a linear decrease in diameter that is continuous from 5 s to 120 s. Diameter versus time plots from each of the 22 measured individual fusions showed six fusion zones as holding their diameters constant from the 5–60 s interval, whereas 16 diameters decreased uniformly and generally in parallel to one another. None of the fusions showed a diameter that continued to increase after the AC field was shifted to zero strength. We do not have flat diaphragm lifetime estimates for these experiments.

Effect of FITC-dextran in the cytoplasmic compartment on the expansion signature

The effect of a protocol to load a ghost with FITC-dextran (from FITC-dextran present externally at 3 or 6 mM) was to produce a population of ghosts heterogeneously labeled at different fluorescence levels. Neither FITC-dextran concentration (3 or 6 mM) seemed to have qualitatively different effects on the appearance, shape, or distribution of the membranes. Sedimentation rates obtained by determining the time-dependent descent of the loaded ghosts revealed that the "brightest" and "medium bright" categories of fluorescent ghost membranes (in 20 mM NaPi) sedimented at 3–12 μm/min (compared with ~80 μm/min for intact swollen erythrocytes in 150–200 mOsmol sucrose (see Abidor et al., 1994) and ~1.5 μm/min for unloaded (pink) ghost membranes in 20 mM NaPi). In other words, sedimentation rates were always proportional to fluorescence levels (data not shown). Most of the fusions of pairs of control (not heat-treated) dextran-loaded ghosts induced by an electric pulse were not accompanied by visually noticeable loss of fluorescence through electroporation (only ~10–25% of all membranes showed noticeable diminution of fluorescence instantaneously upon the application of the electric field pulse). The brightness of the fluorescence in the FITC-loaded ghosts underwent a diminution due to excitation-based bleaching but could not be quantitatively measured because of video noise. However, on the basis of previous work, overall bleaching was visually estimated to be (very approximately) ~20–40%/min with continuous excitation under our conditions. Hence, the recorded data were taken by looking in fusions for any fluorescence diminution upon and after the application of the pulse and, if this was not visually detectable, then switching to phase optics for recording fusion zone diameter expansion. In contrast, fusions of loaded ghosts that were heat-treated led to a much greater loss or a complete loss of fluorescence within a few seconds in a high fraction of the population, and we abandoned additional work. (However, loss of hemoglobin, compared with FITC-dextran, seemed to be more limited according to studies from another laboratory (Miles and Hochmuth, 1987; Miles, 1988), suggesting that this approach could be pursued if a solute of large molecular weight were to be used.)

Previous studies (Dimitrov and Sowers, 1990) showed that an electric field-induced fluorescence diminution would have to be at least 5–7% to be visually perceptible and suggested that in preliminary experiments such as these, the contents of the ghost membrane could be visually considered to be, to a first approximation, essentially constant. Because bleaching, Brownian motion, drift, and pixel-pixel

video noise (caused by a combination of features in the specific apparatus we used) prevented us from making useful quantitative measures of fluorescence, we conducted this part of the study by first scanning a suspension to quickly find two-member ghosts pairs in which both ghosts had at least "medium bright" fluorescence levels. Then we switched to phase optics and fused the pair while recording the fusion zone expansion on videotape. Fig. 6 shows the expansion curve for the 0–5 s period after membrane fusion of nonheat-treated ghosts for fusions in which both ghosts were not loaded compared with fusions in which the ghosts were resealed in the presence of 5 mM FITC-dextran (10 kDa) to provide an osmotically active solute on one side of the membrane (but not from the 20 mM NaPi, pH 8.5, buffer that was already present on both sides of the membrane). It is clear that the fusion of solute-loaded ghost membranes was accompanied by a higher rate of fusion zone expansion in the first 0.5 s. At all times thereafter, the fusion zone diameter, D, in the loaded ghost fusion product seemed to continue to remain a constant ΔD larger than the control group fusion zone diameter.

It must be acknowledged, however, that the presence of the FITC-dextran may have influenced the diameter versus time curves by a mechanism involving the binding to one or more sites on the inside membrane surface rather than by osmotic pressure.

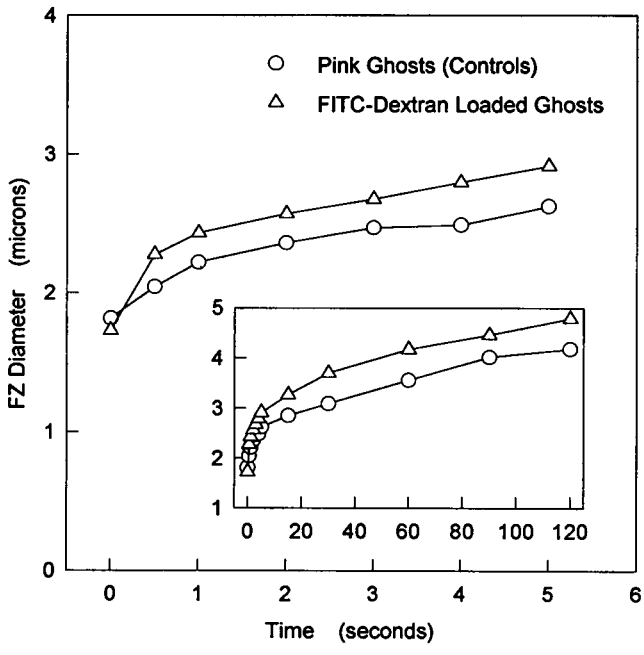

FIGURE 6 Fusion zone expansion signature from 0–5 s after membrane fusion (inset: signature during entire observation interval) in fusions of (nonheat-treated) pairs of control (○), i.e., "pink ghosts," and FITC-dextran (△) loaded ghosts (see Materials and Methods). AC field: 4 V/mm continuous and constant at all times. (△, N = 10; △, N = 21).

Comparing the effect from a net osmotic pressure difference with the effect from a dielectrophoretic force field on the fusion zone expansion signature

The most important new fact in considering the use of the osmotic-based, force-assisted expansion of the fusion zone to calibrate the dielectrophoretic force is the observation that the complete elimination of the AC field at some time after membrane fusion will lead to a contraction of the fusion zone diameter (Fig. 5). This means that at least in heat-treated membranes, fusion zone expansions should normally not take place without an externally provided force or condition (see below). Because all of our previous measurements of fusion zone expansion signatures were done with an AC field that was continuously present at a constant level after membrane fusion was induced, we must first estimate the magnitude of the accelerating effect caused by the presence of the dielectrophoretic force field. The most straightforward first approximation would be to estimate the external dielectrophoretic force, which if produced would hold constant a given fusion zone diameter. Assuming a linear relationship between fusion zone diameter and external microforce (i.e., a Hook's law relationship combined with a viscous element), and asking for the circumstances in which the expansion rate is similar for the two microforces, then an AC field strength that produces a steady state can be obtained by interpolation as follows. From Fig. 5, the expansion (shown by ●) over the $3 < t <$ 30-s interval ended at D = 3.8 μm, after starting from D = 3.3 μm. This is a total distance of +0.5 μm at 4 V/mm. Also, from Fig. 5, the contraction in diameter (shown by ■) during the 5–30 s interval ended with D = 4.0 μm, after starting from D = 4.3 μm, and is −0.3 μm at 0 V/mm field strength. Thus, to a first approximation, a total of 0.5 + 0.3 = 0.8 μm of constant velocity is produced for every 4 V/mm field strength, or 0.8/4 = 0.2 μm/V/mm. Therefore, an AC strength of ~1.5 V/mm would be needed to get a zero rate of expansion at some time after membrane fusion.

Because heat-treated membranes containing FITC-dextran lost fluorescence upon membrane fusion, this comparison will be based only on fusion of control (i.e., not heat-treated) membranes. If we know that the continuous presence of the AC at a constant level (4.0 V/mm) caused fusion zones to expand to a larger diameter in control membranes than in the total absence of AC (from ■ in Fig. 5), we may then consider how much additional diameter expansion was caused in these membranes by the presence of both FITC-dextran and the 4.0 V/mm AC field (Fig. 6). The 0–1 s time interval was chosen in the high (8.0 V/mm) and low (3.5 V/mm) AC field-induced fusion zone expansion data because the data point at 0.5 s seemed to be anomalously higher compared with back extrapolations from either the high or low AC data points for 1, 3, and 5 s (Fig. 7, a replot of the early data in Fig. 3). Numerically, this is (final minus initial) 3.2 − 2.05 = 1.15 μm from N = 14 measurements with E = 8.0 V/mm and 2.9 − 1.92 = 0.98

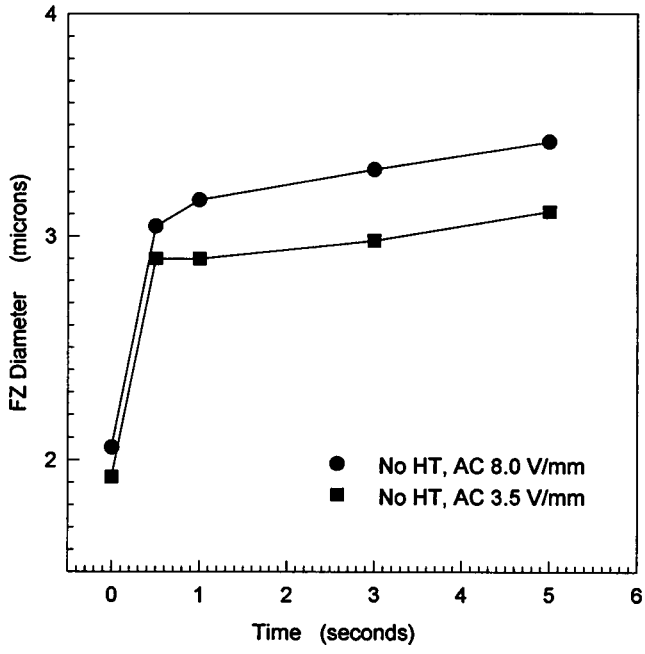

FIGURE 7 Fusion zone expansion signature in fusions of nonheat-treated pairs of control ("pink ghosts") in the continuous presence of a constant low (3.5 V/mm) or high (8.0 V/mm) 60-Hz alternating electric field. Data replotted from 0–5 s in Fig. 3.

μm from $N = 9$ measurements at $E = 3.5$ V/mm. Therefore 8 V/mm provides a 1.15/0.98 = 17% increase over 3.5 V/mm. The FITC-dextran–enhanced expansions of fusion zones in fusions of nonheat-treated ghost during the 0–1 s interval were (final − initial) 2.45 − 1.75 = 0.7 μm/s (N = 21), and in the fusions without FITC-dextran present (controls, N = 10), they were (final − initial) 2.2 − 1.8 = 0.4 μm/s = 1.75 × increase over the controls. An additional diameter increase by 1.17 per 4.5 V/mm, compared with an increase of 0.75 per 5 mM means that 1.0 V/mm of dielectrophoretic field strength has an effect equivalent to ~0.25 mM of osmotic pressure difference. It is acknowledged that an actual force calculation, rather than the force equivalence comparison we made, will require that additional membrane biomechanical factors be taken into consideration. Furthermore, although it is theoretically possible to calculate osmotic pressure, we did not perform this calculation for four reasons. First, we could not make quantitative experimental estimates of solute concentration from the fluorescence of a label because our low-light-level camera, a SIT-68, and the single-frame grabber produced too much video noise, and the software was unable to average out the pixel-pixel noise. Second, we would have desired to independently verify (but could not) the estimates of solute concentration by the sedimentation rate and after membrane fusion was induced. Third, we would require quantitative evidence that insignificant or very small amounts of solute were lost by electroporation at and after the moment that the electric field pulse was applied to induce fusion. These data would be needed because a quantitative calculation would otherwise be uncomfortably close to noise and experimental error. Fourth, although a biomechanical model (using STZC material characteristics) exists for cell fusion (Akkas, 1984), the contribution from surface tension may not be straightforward since discrepancies between methods and models have been reported in the literature (Harvey, 1954, for review).

Implications for cell fusion as induced by viruses

Our findings show that the spectrin-based membrane skeleton, regardless of whether it undergoes the 42°C, 20-min heat treatment, tends to actually prevent the cell rounding that follows membrane fusion. The possibility that the membrane skeleton may be functioning in a manner similar to that found in virus-induced nucleated cell fusions (e.g., in syncytium formation) requires an explanation for the fact that syncytia are commonly found in cultured cells infected with enveloped viruses. One factor is that it is known that a virion-membrane interaction (hemolytic) can alter the permeability (Schlegel, 1987) of the plasma membrane, which could bring about colloid-osmotic swelling, a simple mechanism for generating a force that overcomes the restraining force of the membrane skeleton. A more complex possibility could involve virus-based alteration of the membrane skeleton.

Other relevant observations

Our observation of a decrease in the fusion zone diameter after the complete removal of the dielectrophoresis-induced forces (Fig. 5) has a parallel in a previous study (Miles and Hochmuth, 1987; Miles, 1988). It was shown in that study that one member of a two-member pair of intact erythrocytes, electrofused to each other, could be aspirated into microcapillaries and then expelled. As more volume of one member of the doublet fusion product entered the capillary, the fusion zone diameter became larger. However, when the aspirated volume was expelled from the microcapillary, the fusion zones were observed to undergo a spontaneous and corresponding contraction in diameter, which had a relaxation half-time of ~1–4 s (Fig. 4.11 in Miles, 1988), but was asymptotic rather than linear in our case (Fig. 5). A complicating factor in the prior work is that the fusions were carried out with intact erythrocytes. In intact erythrocytes, electroporation, which is known to take place at fusogenic electric pulse strengths (Tsong, 1991; Sowers, 1995), will at least lead to a complex and transient alteration in the transmembrane ion concentration difference, a consequent loss of membrane potential, and possibly some colloid-osmotic swelling and hemolysis (Kinosita and Tsong, 1977a,b; Ahkong and Lucy, 1986). These multiple effects will disturb the metabolite pool levels and ionic concentrations and could be expected to create or change many forces in an uncontrolled way. Nevertheless, the overriding observation was that fusions of intact cells showed a tendency for fusion zone diameters to shrink after a stretch, which is consistent

with our observations. This suggests that the spectrin-based membrane skeleton may have similar effects in fusions of nucleated cells.

A study of electrofusion of intact erythrocytes, in contrast to the electrofusion of erythrocyte ghosts in our work, has also shown that the expansion of the fusion zone can be perturbed by experimental manipulation of external osmotic pressure (Li and Hui, 1994), although most of that work was directed at measuring fusion yield (= membrane fusion) rather than fusion zone expansion (= cell fusion). However, our work was always limited to erythrocyte ghost membranes because an electric field pulse treatment has also been reported 1) to induce in intact erythrocytes a progressive shape change (Tsong and Kingsley, 1975; Sowers, 1985), 2) to induce colloid-osmotic swelling sometimes leading to hemolysis (Tsong and Kingsley, 1975), and 3) to induce lipid flip-flop (Schwister and Deuticke, 1985). These could lead to disturbances that could affect the processes studied and reported by Li and Hui (1994), who also reported a synergistic enhancement of intact erythrocyte electrofusion yield by polyethylene glycol, which resembles prior reports of the modulation of fusion yield in erythrocyte ghosts (Sowers, 1990) and nucleated cells (Zhang et al. 1991; Lee et al., 1992) by several species of macromolecule. Nevertheless, even though our experimental conditions were different in detail, in general our results are consistent with the results of Li and Hui (1994). However, it must be emphasized that fusion yield and fusion zone expansion kinetics are experimentally separable phenomena.

Although an erythrocyte rounding-up process does not take place at any stage in malaria, it is known that erythrocyte invasion by the parasite that causes the disease will alter the phosphorylation levels of several membrane proteins (Cohen and Gascard, 1992, for review) and, in a cause-effect relationship, rigidify the membrane (Pasvol et al., 1989; Cranston et al., 1984). Furthermore, in as yet uncharacterized processes in nucleated cells, it is known that spectrin is physically relocated during mitosis (Fowler and Adam, 1992), lymphocyte activation (Lee et al., 1988; Gregorio et al., 1992), and growth activation (Bretscher, 1989).

Our observations generate a key question for future work to answer: What is the molecular nature of the spectrin network when it has undergone a heat treatment that has traversed only about half way through the known spectrin calorimetric transition? Some protein unfolding had to occur, but the fusion zone diameter expansion rates are still essentially linear, although at a somewhat higher rate than for fusions of control membranes (Fig. 1 in Wu et al., 1994a). Moreover, why do such treatments lead to relatively small effects on fusion zone diameter expansions but cause such dramatic shortening of flat diaphragm lifetimes? Also, by what mechanism do 2,3-diphosphoglyceric acid and wheat germ agglutinin affect the rate and flat diaphragm lifetime in heat-treated membranes as shown in Wu et al. (1994a). In addition, the higher sensitivity of heat-treated, compared to control, ghost membranes to electroporation is counterintuitive from the point of view that it is known that such heat treatments actually reduce the deformability of erythrocyte membranes (see Wu et al., 1994a, for discussion). We await future experiments to detect parallel effects on nonheat-treated membranes.

Although it is clear that the problem is complex and will require additional work for a more complete analysis, our data indicate that it may be feasible to eventually identify and quantify many if not all of the significant participating force components and to develop a new biomechanics approach.

This work was supported by Office of Naval Research Grant N00014-92-J-1053 and National Institutes of Health Grant R03-RR07764.

I thank Jason D. Rosenberg and Shuxia Quan for technical assistance, and Ken Foster, Leslie Fung, and Anne Haywood for useful discussions.

REFERENCES

Abidor, I. G., and A. E. Sowers. 1994. Kinetics and mechanism of cell membrane electrofusion. *Biophys. J.* 60:1557–1569.

Ahkong, Q. F., and J. A. Lucy. 1986. Osmotic forces in artificially induced cell fusion. *Biochim. Biophys. Acta.* 858:206–216.

Akkas, N. 1984. Biomechanics of virus-to-cell and cell-to-cell fusion. *J. Biomed. Eng.* 6:257–264.

Bennett, V. 1990. Spectrin-based membrane skeleton: a multipotential adaptor between plasma membrane and cytoplasm. *Physiol. Rev.* 70: 1029–1065.

Bessis, M. 1973. Living Blood Cells and Their Ultrastructure. Springer Verlag, New York.

Bretscher, A. 1989. Rapid phosphorylation and reorganization of ezrin and spectrin accompany morphological changes induced in A-431 cells by epidermal growth factor. *J. Cell Biol.* 108:921–930.

Chasis, J. A., and N. Mohandas. 1986. Erythrocyte membrane deformability and stability: two distinct membrane properties that are independently regulated by skeletal protein associations. *J. Cell Biol.* 103: 343–350.

Chasis, J. A., N. Mohandas, and S. B. Shohet. 1985. Erythrocyte membrane rigidity induced by glycophorin A-ligand interaction. Evidence for a ligand-induced association between glycophorin A and skeletal proteins. *J. Clin. Invest.* 75:1919–1926.

Chernomordik, L. V., and A. E. Sowers. 1991. Evidence that the spectrin network and a nonosmotic force control the fusion product morphology in electrofused erythrocyte ghosts. *Biophys. J.* 60:1026–1037.

Cohen, C. M., and Gascard, P. 1992. Regulation and post-translational modification of erythrocyte membrane and membrane-skeletal proteins. *Semin. Hematol.* 29:244–292.

Cranston, H. A., C. W. Boylan, G. L. Carroll, S. P. Sutera, J. R. Williamson, I. Y. Gluzman, D. J. Krogstad. 1984. *Plasmodium falciparum* maturation abolishes physiologic red cell deformability. *Science.* 223: 400–403.

de Rijter, N., and A. Emons. 1993. Immunodetection of spectrin antigens in plant cells. *Cell Biol. Int. Rept.* 17:169–182.

Deuticke, B. 1968. Transformation and restoration of biconcave shape of human erythrocytes induced by amphiphilic agents and changes of ionic environment. *Biochim. Biophys. Acta.* 163:494–500.

Dimitrov, D. S., and A. E. Sowers. 1990. Membrane electroporation: fast molecular exchange by electroosmosis. *Biochim. Biophys. Acta.* 1022: 381–392.

Duzgunes, N. 1993a. Membrane Fusion Techniques, Part A. *Methods Enzymol.* Vol. 220. Academic Press, San Diego. 1–433.

Duzgunes, N. 1993b. Membrane Fusion Techniques, Parts B. *Methods Enzymol.* Vol. 221. Academic Press, San Diego. 1–464.

Elgsaeter, A., B. T. Stokke, A. Mikkelsen, and D. Branton. 1986. The molecular basis of erythrocyte shape. *Science.* 234:1217–1223.

Foster, K. R., and A. E. Sowers. 1995. Dielectrophoretic forces and potentials induced on pairs of cells in an electric field. *Biophys. J.* 69:777–784.

Fowler, V. M., and E. J. H. Adam. 1992. Spectrin redistributes to the cytosol and is phosphorylated during mitosis in cultured cells. *J. Cell Biol.* 119:1559–1572.

Gregorio, C. C., R. T. Kubo, R. B. Bankert, and E. A. Repasky. 1992. Translocation of spectrin and protein kinase C to a cytoplasmic aggregate upon lymphocyte activation. *Proc. Natl. Acad. Sci. USA.* 89: 4947–4951.

Grimaila, R. J., B. A. Fuller, P. D. Rennert, M. B. Nelso, M.-L. Hammarksjold, B. Potts, M. Murray, S. D. Putney, and G. Gray. 1992. Mutations in the principal neutralization determinant of human immunodeficiency virus type 1 affect syncytium formation, virus infectivity, growth kinetics, and neutralization. *J. Virol.* 66:1875–1883.

Harvey, E. N. 1954. Tension at the cell surface. *Protoplasmatologia.* 16:1–30.

Haywood, A. M. 1991. Evidence for multiple steps in enveloped virus binding. *In* Cell and Model Membrane Interactions. S. Ohki, editor. Plenum Press, New York. 149–162.

Horvath, C. M., R. G. Paterson, M. A. Shaughnessy, R. Wood, and R. A. Lamb. 1992. Biological activity of paramyxomirus fusion proteins: factors influencing formation of syncytia. *J. Virol.* 66:4564–4569.

Kemble, G. W., T. Danielli, and J. White. 1994. Lipid-anchored influenza hemagglutinin promotes hemifusion, not complete fusion. *Cell.* 76: 383–391.

Kinosita, K., and T. Y. Tsong. 1977a. Voltage-induced pore formation and hemolysis of human erythrocytes. *Biochim. Biophys. Acta.* 471: 227–242.

Kinosita, K., and T. Y. Tsong. 1977b. Formation and resealing of pores of controlled sizes in human erythrocyte membrane. *Nature.*268:438–441.

Knutton, S. 1977. Studies of membrane fusion. II. Fusion of human erythrocytes by sendai virus. *J. Cell Sci.* 28:189–210.

Knutton, S., and C. A. Pasternak. 1979. The mechanism of cell-cell fusion. *Trends Biochem. Sci.* 4:220–223.

Lee, J. K., J. D. Black, E. A. Repasky, R. T. Kubo, and R. B. Bankert. 1988. Activation induces a rapid reorganization of spectrin in lymphocytes. *Cell.* 55:807–816.

Lee, R. C., L. P. River, F.-S. Pan, L. Ji, and R. L. Wollmann. 1992. Surfactant-induced sealing of electropermeabilized skeletal muscle membranes in vivo. *Proc. Natl. Acad. Sci. USA.* 89:4524–4528.

Li, L.-H., and S.-W. Hui. 1994. Characterization of PEG-mediated electrofusion of human erythrocytes. *Biophys. J.* 67:2361–2366.

Lucy, J. A. 1978. Mechanisms of chemically induced cell fusion. *In* Cell Surface Reviews: Membrane Fusion, Vol 5. G. Poste and G. L. Nicolson, editors. Elsevier North-Holland Biomedical Press, Amsterdam. 268–304.

Miles, D. M. 1988. Investigation of electrofused erythrocytes by pipette micromanipulation. Dissertation. Duke University, Durham, NC.

Miles, D. M., and R. M. Hochmuth. 1987. Micromanipulation and elastic response of electrically fused red cells. *In* Cell Fusion. A. E. Sowers, editor. Plenum, New York. 441–456.

Monck, J. R., G. Alvarez de Toledo, and J. M. Fernandez. 1990. Tension in secretory granule membranes causes extensive membrane transfer through the exocytotic fusion pore. *Proc. Natl. Acad Sci. USA.* 87: 7804–7808.

Monck, J. R., A. F. Oberhauser, G. Alvarez de Toledo, and J. M. Fernandez. 1991. Is swelling of the secretory granule matrix the force that dilates the exocytotic fusion pore? *Biophys. J.* 59:39–47.

Oberhauser, A. R., J. R. Monck, and J. M. Fernandez. 1992. Events leading to the opening and closing of the exocytotic fusion pore have markedly different temperature dependencies: kinetic analysis of single fusion events in patch-clamped mouse mast cells. *Biophys. J.* 61:800–809.

Palek, J., and S. E. Lux. 1983. Red cell membrane skeletal defects in hereditary and acquired hemolytic anemias. *Semin. Hematol.* 20: 189–224.

Pasvol, G., J. A. Chasis, N. Mohandas, D. J. Anstee, M. J. A. Tanner, and A. H. Merry. 1989. Inhibition of malarial parasite invasion by monoclonal antibodies against glycophorin A correlates with reduction in red cell membrane deformability. *Blood.* 74:1836–1843.

Pinto da Silva, P., K. Shimizu, and C. Parkison. 1980. Fusion of human erythrocytes induced by sendai virus: freeze-fracture aspects. *J. Cell Sci.* 43:419–432.

Poste, G., and G. L. Nicolson. 1978. Cell Surface Reviews: Membrane Fusion, Vol. 5. Elsevier/North Holland Biomedical Press, Amsterdam. 1–862.

Roizman, B. 1962. Polykaryocytosis. *Cold Spring Harbor Symp. Quant. Biol.* 27:327–342.

Schlegel, R. 1987. Probing the function of viral fusion proteins with synthetic peptides, *In* Cell Fusion, A. E. Sowers, editor. Plenum, New York. 33–43.

Schwister, K., and B. Deuticke. 1985. Formation and properties of aqueous leaks induced in human erythrocytes by electrical breakdown. *Biochim. Biophys. Acta.* 816:332–348.

Song, L., Q. F. Ahkong, D. Georgescauld, and J. A. Lucy. 1991. Membrane fusion without cytoplasmic fusion (hemi-fusion) in erythrocytes that are subjected to electrical breakdown. *Biochim. Biophys. Acta.* 1065:54–62.

Sowers, A. E. 1983. Fusion of mitochondrial inner membranes by electric fields produces inside-out vesicles: visualization by freeze-fracture electron microscopy. *Biochim. Biophys. Acta.* 735:426–428.

Sowers, A. E. 1985. Movement of a fluorescent lipid label from a labeled erythrocyte membrane to an unlabeled erythrocyte membrane following electric-field-induced fusion. *Biophys. J.* 47:519–525.

Sowers, A. E. 1986. A long-lived fusogenic state is induced in erythrocyte ghosts by electric pulses. *J. Cell Biol.* 102:1358–1362.

Sowers, A. E. 1988. Fusion events and nonfusion contents mixing events induced in erythrocyte ghosts by an electric pulse. *Biophys. J.* 54: 619–625.

Sowers, A. E. 1989. The mechanism of electroporation and electrofusion in erythrocyte membranes. *In* Electroporation and Electrofusion in Cell Biology. E. Neumann, A. E. Sowers, and C. A. Jordan, editors. Plenum Publishing, New York. 229–256.

Sowers, A. E. 1990. Low concentrations of macromolecular solutes significantly affect electrofusion yield in erythrocyte ghosts. *Biochim. Biophys. Acta.* 1025:247–251.

Sowers, A. E. 1992. Mechanisms of electroporation and electrofusion in erythrocyte membranes. *In* Guide to Electroporation and Electrofusion. D. C. Chang, B. M. Chassy, J. A. Saunders, and A. E. Sowers, editors. Academic Press, San Diego. 119–138.

Sowers, A. E. 1993. Membrane electrofusion: a paradigm for study of membrane fusion mechanisms. *Methods Enzymol.* 220:196–210.

Sowers, A. E. 1995. Permeability alteration by transmembrane electric fields: electroporation. *In* Permeability and Stability of Lipid Bilayers. E. A. Disalvo and S. A. Simon, editors. CRC Press, Boca Raton. 105–121.

Spruce, A. E., A. Iwata, and W. Almers. 1991. The first milliseconds of the pore formed by a fusogenic viral envelope protein during membrane fusion. *Proc. Natl. Acad. Sci. USA.* 88:3623–3627.

Tsong, T. Y. 1991. Electroporation of cell membranes. *Biophys. J.* 60: 297–306.

Tsong, T. Y., and E. Kingsley. 1975. Hemolysis of human erythrocyte induced by a rapid temperature jump. *J. Biol. Chem.* 250:786–789.

White, J. 1992. Membrane fusion. *Science.* 258:917–924.

Wojcieszyn, J. W., R. A. Schlegel, K. Lumley-Sapanski, and K. A. Jacobson. 1983. Studies on the mechanism of polyethylene glycol-mediated cell fusion using fluorescent membrane and cytoplasmic probes. *J. Cell Biol.* 96:151–159.

Wu, Y.-K., J. D. Rosenberg, and A. E. Sowers, 1994a. Surface shape change during fusion of erythrocyte membranes is sensitive to membrane skeleton agents. *Biophys. J.* 67:1896–1905.

Wu, Y.-K., R. A. Sjodin, and A. E. Sowers. 1994b. Distinct mechanical relaxation components in pairs of erythrocyte ghosts undergoing fusion. *Biophys. J.* 66:114–119.

Zhang, L., U. Fiedler, and H. Berg. 1991. Modification of electrofusion of barley protoplast by membrane-active agents. *Bioelectrochem. Bioenerg.* 26:87–96.